Table 1. Top ranked typhoons that bring great amount of total rainfall recorded at the 3 rain gages nearby the Chenyulan watershed

Rain gage	Sun Moon Lake			Mt. Ali			Mt. Jade		
Rank	Year/Typhoon Name		Total rainfall (mm)	Year/Typhoon Name		Total rainfall (mm)	Year/Typhoon Name		Total rainfall (mm)
1	2008	SINLAKU	854.1	2009	MORAKOT	3059.5	2009	MORAKOT	2160.8
2	1960	SHIRLEY	721.7	1996	HERB	1987	2005	HAITANG	1144.5
3	2009	MORAKOT	706.5	2008	SINLAKU	1457.7	2008	SINLAKU	881.5
4	1996	HERB	652.9	1963	GLORIA	1433.5	1990	YANCY	718.5
5	1963	GLORIA	568	2005	HAITANG	1215.5	1996	HERB	710.5
6	2008	KALMAEGI	555	1990	YANCY	1194	2004	MINDULLE	702.6
7	1994	DOUG	551.9	2004	MINDULLE	1181.5	1963	GLORIA	696.5
8	2012	SAOLA	512.5	1966	TESS	1104.6	2004	AERE	651.5
9	1990	YANCY	505.5	2007	KROSA	1093	2005	MATSA	635.5
10	2005	MATSA	493.2	1960	SHIRLEY	1091.2	1989	SARAH	595.4

Image Analysis

In this study, we applied the image process software, ERDAS IMAGE for land use/cover data of 2008-2013. In order to evaluate the impact of large-scale disturbances on the ecosystem, we collected SPOT images taken after each disturbance event. The SPOT images were purchased from the Space and Remote Sensing Research Center and used for watershed land cover classification for 2008/11/28, 2009/12/2, 2010/11/21, 2011/9/22, 2012/10/25, and 2013/11/15 after typhoons. Four major steps for the image process include coordinate system projection, radiative correction, supervised classification, and accuracy assessment. The criteria used for judging the accuracy of final SPOT images are the all accuracies and kappa values exceeding 85% and 0.8, respectively.

SWAT Model

The Soil and Water Assessment Tool (SWAT) model was used to estimate the impact of historical land use/cover and climate conditions on ecosystem services of the Chenyulan watershed. The model can predict long-term impacts of land use and management on water, sediment and agricultural chemical yields at different scales in a mixed land use watershed (Arnold et al., 1998). The major GIS input files for the SWAT model are the digital elevation model (DEM) at 30 m resolution (processed by Center for GIS, RCHSS, Academia Sinica, Taiwan, 2012), land use/cover and soil data. The land use maps for the years 2008-2013 were developed using SPOT images. The watershed was delineated into 28 subbasins based on the DEM, specification of streams and inlets/outlets. Then the subbasins were portioned into homogeneous units (hydrologic response units, HRUs) by setting 0% threshold percentages of land use, soil type and slope. Weather data (daily precipitation, minimum and maximum

temperature) were obtained from Sun Moon Lake, Mt. Ali and Mt. Jade stations within or nearby the Chenyulan watershed. Other weather variables needed by the model (solar radiation, wind speed and relative humidity) were estimated using the weather generator built into the SWAT model (Fig. 2.).

Three statistical criteria were used in this study to evaluate the model performance on monthly streamflow and total suspended sediment (TSS) losses. They are coefficient of determination (R^2), Nash-Sutcliffe efficiency (NSE) and percent bias (PBIAS).

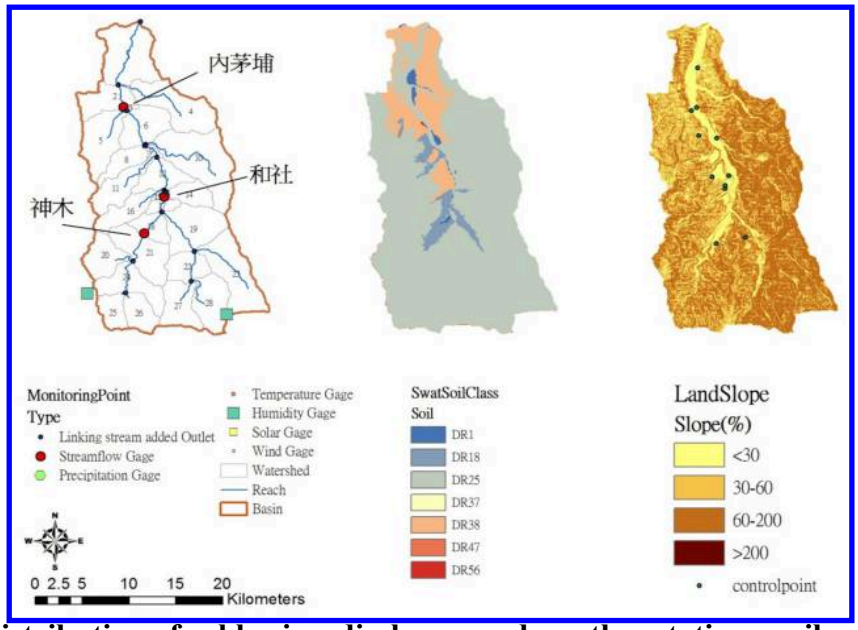

FIG. 2. Distribution of subbasins, discharge and weather stations, soil and slope.

RESULTS

Image Process Results

We selected 11 control points, including the sport fields of 7 elementary schools, one police office and 3 road sections, for radiative correction. There are 4 imagery files representing Band 1 (Green), Band 2 (Red), Band 3 (Near infra-red, NIR) and Band 4 (Short-wave infra-red, SWIR). Four different band values of control points of each year were first compared with those of the selected base year (2008-2013). Based on the regression analysis between any two years, we found that the band values of the control points of the year of 2010 had better R^2 values with those of the other years, especially for Band 1, Band 2 and Band4. Thus, the radiative correction based on the regression equations was completed by using year 2010 as the correction base year. By further using the supervised classification method, the images of year 2008-2013 were reclassified into 7 land use/cover classes (Table 2). The kappa values for 2008-2013 images are between 0.67-.072, indicating general accuracy of image classification. During 2008-2013, both riparian and cultivated lands were decreased from 7.09 to 5.71 km^2 and from 23.35% to 7.33%, respectively. The increase in landslide areas in 2011 (5.25%) and 2013 (4.26%) indicated the cumulative impacts of natural disturbances (i.e., typhoons) on the watershed. However, there was no significant trend of change in grass land and forest, which may be the reclassification errors due to the time at different stages of plant growth when the images were taken (Fig. 3).

Table 2. Land use/cover during 2008-2013 in the Chenyulan watershed (km^2, %)

	2008	2009	2010	2011	2012	2013
Riparian	7.09 (1.58%)	6.47 (1.44%)	12.07 (2.69%)	16.51 (3.68%)	7.24 (1.61%)	5.71 (1.27%)
Grass	44.7 (9.96%)	25.64 (5.71%)	34.70 (7.73%)	19.06 (4.25%)	23.51 (5.24%)	20.51 (4.57%)
Buildup	8.75 (1.95%)	12.59 (2.81%)	11.40 (2.54%)	20.67 (4.61%)	11.59 (2.58%)	11.19 (2.49%)
Cultivated land	63.58 (14.17%)	104.81 (23.35%)	77.43 (17.25%)	87.56 (19.51%)	79.69 (17.75%)	32.88 (7.33%)
River sand	5.57 (1.24%)	8.35 (1.86%)	2.34 (0.52%)	2.97 (0.66%)	6.60 (1.47%)	4.51 (1.01%)
Landslide	12.76 (2.84%)	17.32 (3.86%)	15.13 (3.37%)	23.57 (5.25%)	15.58 (3.47%)	19.10 (4.26%)
Forest	306.36 (68.26%)	273.63 (60.97%)	295.75 (65.9%)	278.46 (62.04%)	304.60 (67.87%)	354.91 (79.08%)

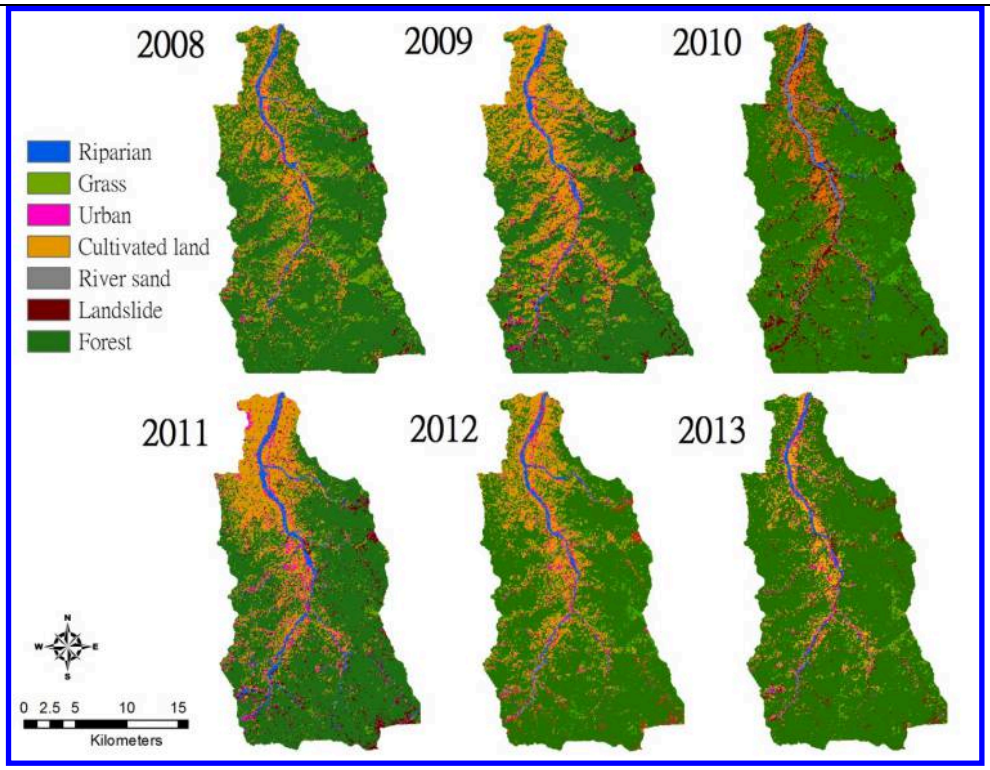

FIG. 3. Land use distribution during 2008-2013 in the Chenyulan watershed.

SWAT Model Results

There are 3 stream gages (Neimoupu, Hesheu, and Shunmu) in this watershed (Fig. 2). However, their available observed data are limited after 1996 due to the gages might be destroyed by severe rainfall or landslides at higher mountain areas. In order to fully capture the model's capability of accurately simulating streamflow and sediment losses, we used the observed data at those three gages from 1990 to 2006 for model calibration and data at Neimoupu station from 2003 to 2013 were used for model validation. Based on the sensitivity analysis, a total of 14 flow-related parameters were calibrated for the whole watershed by using the SWAT calibration model, SWAT-CUP. Followed by the flow calibration, 8 sediment-related parameters

were calibrated for the monthly TSS loads at three gages. It should be noted that most of the calibrated parameter values were applied for the whole watershed, except CN (curve number), ALPHA_BF (baseflow alpha factor), GW_DELAY (groundwater delay time), and USLE_P (soil evaporation compensation factor) were calibrated specifically for different subbasins that drain to each gage. The model performed satisfactory (R^2 >0.5, NSE>0.5, and -25% <PBIAS<25%) (Moriasi et al., 2007) for monthly streamflow at Neimoupu (R^2=0.65, NSE=0.6, PBIAS=4.5%), Hesheu (R^2=0.68, NSE=0.66, PBIAS=12.2%), and Shunmu (R^2=0.73, NSE=0.73, PBIAS=4.5%) (Fig. 4). However, the model needs to be further improved for simulating monthly TSS loads (Fig. 5).

By comparing the simulation results of different years of land use/cover with that of 1996, the difference can be regarded as the cumulative natural disturbance impacts on the watershed ecosystem services, especially the upstream areas where landslide frequently occurs during typhoons (Table 3).

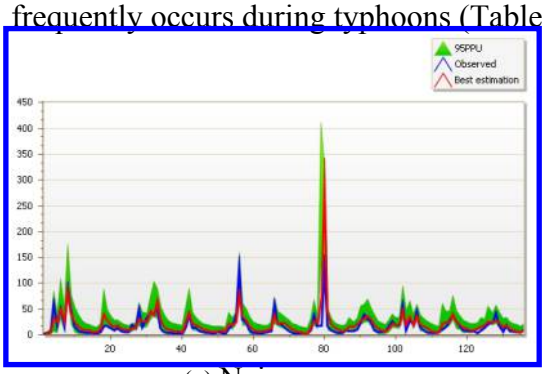

(a) Neimoupu

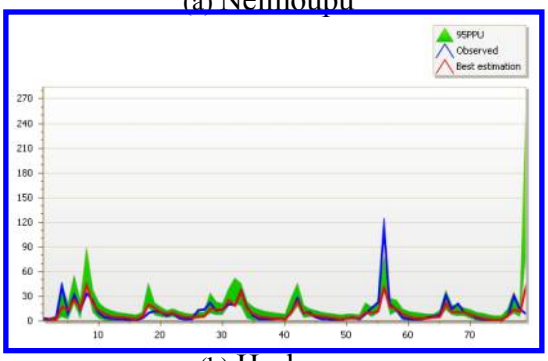

(b) Hesheu

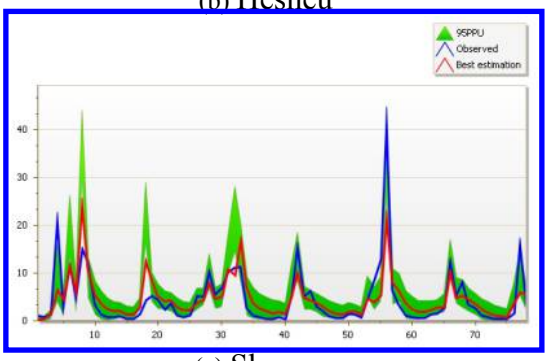

(c) Shunmu

FIG. 4. Comparison of observed and simulated monthly streamflow (cms)

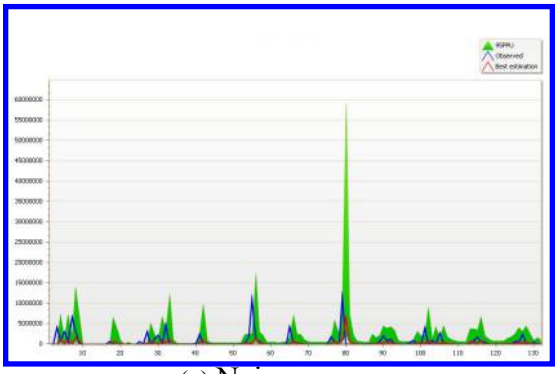

(a) Neimoupu

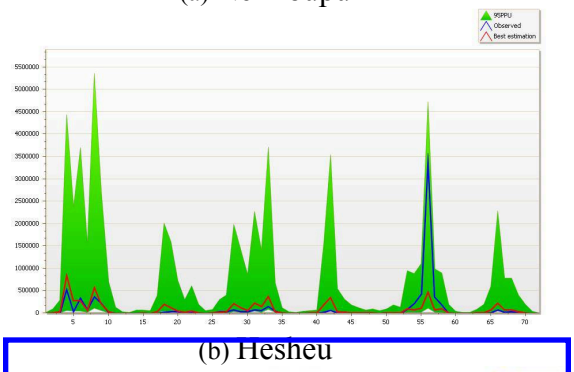

(b) Hesheu

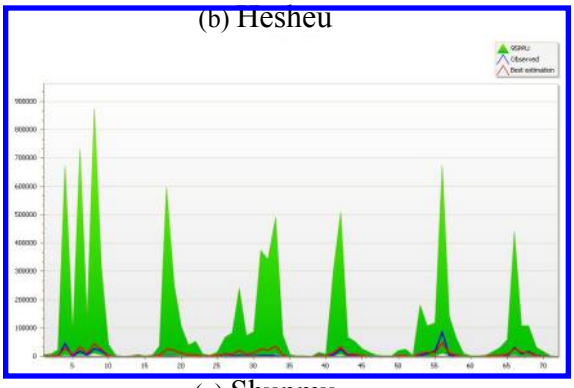

(c) Shunmu

FIG. 5. Comparison of observed and simulated monthly TSS (Tons/day)

Table 3. Land use/cover impacts on streamflow and TSS at Neimoupu

Year of land use/cover	FLOW(cms)	TSS(tons)	Diff. in flow (%)	Diff. in TSS (%)
1996	20.08	4068080	-	-
9903	20.03	4043875	-0.21	-0.59
9910	20.12	4023290	0.22	-1.10
2000	20.11	4150170	0.18	2.02
2001	20.21	4217580	0.67	3.67
2004	20.20	4207790	0.60	3.43
2005	20.26	4159000	0.91	2.23
2008	20.68	4595920	3.03	12.98
2009	21.08	4880580	4.98	19.97
2010	20.82	4661540	3.70	14.59
2011	20.98	4383920	4.52	7.76
2012	20.72	4523040	3.19	11.18
2013	20.32	4160830	1.23	2.28

CONCLUSIONS

The main goal of this study was to quantify the cumulative impacts of natural disturbances on watershed ecosystem services (i.e., streamflow amount, TSS retention) during 2008-2013. The image classification results showed that there are some areas mis-reclassified due to the time at different plant growth season when the satellite images were taken. Generally, it was found that landslide areas have increased due to the cumulative impacts of typhoons since the study year 2008, especially in the upstream mountain areas where landslides easily occur. Furthermore, based on the simulation results the cumulative impacts of typhoons until 2009 were the most in terms of an increase in TSS loads by 19.97% compared to the simulated TSS loads under 1996 land use/cover condition. Further model calibration and validation are needed in order to obtain more accurate simulation results for assisting the watershed management planning in the Chenyulan watershed.

ACKNOWLEDGMENTS

The authors appreciate the Ministry of Science and Technology, R.O.C. for financially supporting this research under the Project No. NSC 103-2313-B-239-001-MY2.

REFERENCES

1. Arnold, J. G., Srinivasan, R., Muttiah, R. S., and Williams, J. R. (1998). “Large area hydrologic modeling and assessment part I: Model development.” *Journal of the American Water Resources Association*, Vol.34 (1): 73-89.
2. Bai, Y., Ouyang, Z., Zheng, H., Li, X., Zhuang, C., and Jiang, B. (2012). “Modeling soil conservation, water conservation and their tradeoffs: A case study in Beijing.” *Journal of Environmental Sciences*, Vol.24 (3): 419-426.
3. Betrie, G. D., Mohamed, Y. A., van Griensven, A., and Srinivasan, R. (2011). “Sediment management modelling in the Blue Nile Basin using SWAT model.” *Hydrol. Earth Syst. Sci.*, 15: 807–818, doi:10.5194/hess-15-807-2011.
4. Brouwer, R., Tesfaye, A. & Pauw, P. (2011). Meta-analysis of institutional-economic factors explaining the environmental performance of payments for watershed services.” *Environmental Conservation*, 38(4): 1-13.

5. Bossa, A. Y., Diekkrüger, B., Giertz, S., Steup, G., Sintondji, L. O., Agbossou, E. K., Hiepe, C. (2012). "Modeling the effects of crop patterns and management scenarios on N and P loads to surface water and groundwater in a semi-humid catchment (West Africa)." *Agricultural Water Management,* 115: 20-37.
6. Chiang, L. C., Lin, Y. P., Huang, T., Schmeller, D. S., Verburg, P. H., Liu, Y. L., and Ding, T.S. (2014). "Simulation of ecosystem service responses to multiple disturbances from an earthquake and several typhoons." *Landscape and Urban Planning*. Vol.122: 41-55.
7. Goldstein, J. H., Caldarone, G., Duarte, T. K., Ennaanay, D., Hannahs, N., Mendoza, G., Polasky, S., Wolny, S., and Daily, G. C. (2012). "Integrating ecosystem-service tradeoffs into land-use decisions." *Proceedings of the National Academy of Sciences*, Vol.109 (19): 7565-7570.
8. Hotchkiss, R. H., Jorgensen, S. F., Stone, M. C., and Fontaine, T. A. (2000). "Regulated river modeling for climate change impact assessment the Missouri river." *Journal of the American Water Resources Association*, Vol.36 (2): 375-386.
9. Moriasi, D. N., J.G. Arnold, M.W. Van Liew, R.L. Bingner, R.D. Harmel, and T.L. Veith, (2007). "Model evaluation guidelines for systematic quantification of accuracy in watershed simulations." *Transactions of the ASABE,* 50 (3): 885-900.
10. Notter, B., Hurni, H., Wiesmann, U., and Abbaspour, K. C. (2012). "Modelling water provision as an ecosystem service in a large East African river basin." *Hydrol. Earth Syst. Sci.*, 16: 69–86, doi:10.5194/hess-16-69-2012.
11. Oeurng, C., Sauvage, S., and Sánchez-Pérez, J. M. (2011). "Assessment of hydrology, sediment and particulate organic carbon yield in a large agricultural catchment using the SWAT model." *Journal of Hydrology*, Vol.401 (3): 145-153.
12. Vigerstol, K. L., and Aukema, J. E. (2011). "A comparison of tools for modeling freshwater ecosystem services." *Journal of environmental management*, Vol.92 (10): 2403-2409.
13. Wurbs, R. A., Muttiah, R. S., and Felden, F. (2005). "Incorporation of climate change in water availability modeling." *Journal of Hydrologic Engineering* 10.5: 375-385.
14. Zhao, B., Kreuter, U., Li, B., Ma, Z., Chen, J., and Nakagoshi, N. (2004). "An ecosystem service value assessment of land-use change on Chongming Island, China." *Land Use Policy*, Vol.21 (2): 139-148.

Sensitivity and Uncertainty Analyses of the Translational Slide at the Cidu Section, 3.1k of the Taiwan Formosan Freeway

Shong-Loong Chen[1]; Chia-Pang Cheng[2]; and Meen-Wah Gui[3]
[1]Professor, Dept. of Civil Engineering, National Taipei Univ. of Technology, 1, Sec. 3, Zhongxiao E. Rd., Taipei 10608, Taiwan. E-mail: f10391@ntut.edu.tw
[2]Ph.D. Student, Dept. of Civil Engineering, National Taipei Univ. of Technology, 1, Sec. 3, Zhongxiao E. Rd., Taipei 10608, Taiwan. E-mail: cheng.jiabang@gmail.com
[3]Professor, Dept. of Civil Engineering, National Taipei Univ. of Technology, 1, Sec. 3, Zhongxiao E. Rd., Taipei 10608, Taiwan. E-mail: mwgui@ntut.edu.tw

Abstract: Long-term water immersion weakens slope rocks and degrades rock-layer parameters such as cohesion (c) and friction angle (φ), causing slope failure. The traditional analyses of slope failure generally set fixed values to the required parameters by limit equilibrium, but omit uncertainties of the parameters. These methods fail to fully reflect the slope safety factor, causing unreliable calculated safety factors. We examined the collapse of the Cidu section (3K+100) dip slope on Taiwan Formosa Freeway for the sensitivity analysis of c and φ and uncertainties related to the variation of the safety factor before and after water immersion and slope rock weakening. The sensitivity analysis results showed that c has greater effects on the slope safety factor compared with φ. In the uncertainty analysis, we used three different point estimate methods and the Monte Carlo simulation to calculate the corresponding slope safety factors. This method established the probabilistic analysis of slope stability. We also explored the effect of ρ (correlation coefficient of c and tan φ) on safety factors. The traditional analysis results found that the factor of safety is approximately 1, but the probability of failure of slopes reaches 50%, indicating urgency in using stabilizing measures.

INTRODUCTION

A huge landslide causes major loss to economy and human life. The occurrence of landslides depends on various types of uncertainties; hence, sensitivity and uncertainty analyses are conducted to calculate probabilistic analysis of slope stability, which cause landslides(e.g., Cassidy et al. 2008; Cho 2009; Fenton and Griffith 2010; Srivastava and Babu 2009; Wang et al. 2011; J. Zhang et al. 2009).

The slope stability analysis methods proposed in this study comprise limit equilibrium analysis and limit analysis. Limit analysis requires identification of the stress–strain relation of the slope material, which is too complex to grasp; hence, traditional engineering mainly uses limit equilibrium analysis for slope stability analysis. Slope stability analysis is often represented by a factor of safety (FS). This

can be expressed in different ways such as the intensity ratio of the anti-sliding shear stress to the sliding shear stress for the sliding surface on most infinite slopes, the anti-sliding force to the sliding force on finite slopes, or the anti-sliding moment to the sliding moment on arc sliding slopes(Christian, Ladd, & Baecher, 1994). The slope height ratio can also be applied, i.e., the ratio of the critical slope height calculated using a theoretical formula to the actual slope height, as well as the method of strength reduction. If we consider all these representations, *FS* can be represented by the ratio of the anti-sliding factor to sliding factor on sliding surfaces:

$$FS = \frac{R}{D}, R = resistance\ factor, D = sliding\ factor \quad (1)$$

If $FS > 1$, the slope is stable; if FS < 1, the slope's instability will cause sliding or collapse. Almost all analytical models fail to consider the uncertainties of variables or parameters. For example, the resistance and sliding factors contain many objective and subjective uncertainties; hence, collapse or sliding could occur even though a slope has $FS > 1$.

Thus, a "safe design" based on a traditional FS may not accurately indicate "safety." The reliability analysis model, which considers the effect of the variance of each variable or parameter, can be used to calculate the *Pf*, reliability index (*RI*), or safety index (*SI*). This is a better way to determine the degree of slope safety and reliability, which could help in issuing reliable warnings.

We use the failure of the Cidu section (3K + 100) dip slope on Taiwan Formosan Freeway as a case study. Our study aims to establish a slope model consistent with field conditions (without considering external forces and anchor reinforcement) in an attempt to explore the variations of slope safety factor and variability of rock slope parameters (γ, c, and φ) before and after immersion and weakening of slope rocks. We use three different point estimate methods (Rosenblueth's, Harr's, and modified Harr's) of probability analysis and the Monte Carlo method to explore the effect of parameter uncertainty on slope stability. We also use this method to establish the reliability of slope sliding and Pf of slopes, and finally explore the effect of the correlation coefficient of the rock parameters c, tan φ, and ρ on the safety factor.

Case Description

A severe slope failure occurred at the Cidu section (3K + 100) of Taiwan Formosan Freeway on April 25, 2010 (see Fig. 1). The local rocks are sedimentary rocks and comprise early Miocene Talio and middle Miocene Shihti formations, both of which strike NE–NNE and tilt southeastward. A geological cross-section of the strata is shown in Fig. 2. The slide occurred mainly along thin interbeds and thin laminae of sandshale. The slope failure is approximately 185 m long from the collapse source to freeway slope and approximately 155 m wide at the bottom. The collapse source fell by 15.8 m from approximately 161.5 to 145.7 m, resulting in a damaged area of 14,000 m^2.

The landslide occurred at the Cidu section (3K+100) of Formosan Freeway on April 25, 2010. The following year, the Ministry of Transportation and Communications presented a report(MOTC R.O.C., 2010) on the disaster. The shear strength parameters of the rocks on the site of the dip-slope slide at the Cidu section (3K+100) of Taiwan Formosan Freeway are listed in Table 1.

FIG. 1. Large-scale landslides on a dip slope at Taiwan Formosan Freeway

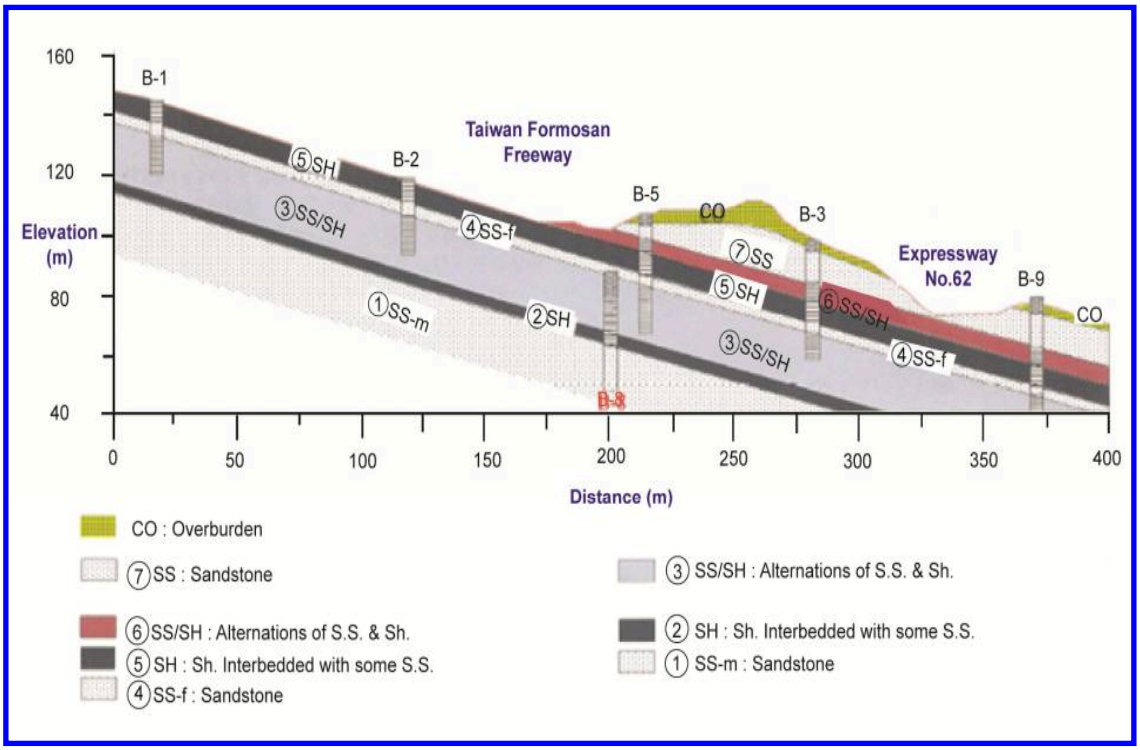

FIG. 2. Geological cross-section perpendicular to the freeway (MOTC R.O.C. 2010)

Table 1. Shear strength parameters

No.	Hole No.	Depth (m)	normal stress (kg/cm^2)	peak strength		residual strength	
				Cp (kg/cm^2)	*Øp (degree)*	*Cr* (kg/cm^2)	*Ør (degree)*
RDS(D)-4	B-6	16.60-17.00	2.0/5.0/7.0	0.28	22.5	0.0	19.8
RDS(D)-5	B-7	18.00-19.00	2.0/4.0/5.0/6.0	3.2	28.5	0.0	22.7
RDS(W)-3	B-3	16.60-17.00	2.0/5.0/7.0	0.9	27.7	0.0	23.2
RDS(W)-4	B-5	16.60-17.00	2.0/3.0/5.0/7.0	1.1	26.2	0.0	14.1

Establishment of Slope Failure Model

The landslide at the Cidu section (3K+100) of Taiwan Formosan Freeway is mainly a dip-slope failure caused by sliding between sandshale strata. We conducted lateral sliding analysis and simulations as shown in Fig. 3, which is described below:

$$FS = \frac{Resistance}{Driving\ force} = \frac{2csin\beta}{\gamma Hsin(\beta-\theta)sin\theta} + \frac{tan\varphi}{tan\beta} \quad (2)$$

$$Probability\ of\ failure\ Pf = FS(c,\phi,\gamma) - 1 < 0$$

This study established the parameters for the slope model by simulating the landslide disaster at 3.1 km on Taiwan Formosan Freeway with reference to the MOTC report (2011). We consider the variability of all the formation parameters, γ, c, and φ, except for the slope height H = 25 m, the sliding surface inclination, and the slope angle. The parameters of the slope failure model thus established are listed in Table 2.

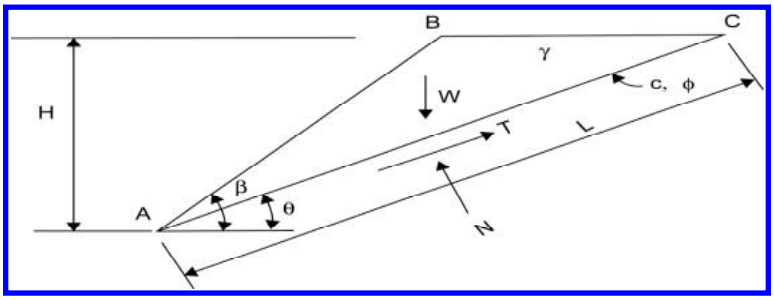

FIG. 3 Parallel sliding surfaces of finite slopes

Table 2. The parameters of the slope failure model

Parameter	Mean	Standard Deviation	Distribution	Remarks
γ **(kn/m3)**	22.9	0.11	Normal distribution	
Cp **(kn/m2)**	2.8-32		Uniform distribution	Before immersion (peak strength)
Cr **(kn/m2)**	0		Constant	After immersion (residual strength)
φp **(degree)**	26.1	2.23	Normal distribution	Before immersion (peak strength)
φr **(degree)**	19.95	3.62	Normal distribution	After immersion (residual strength)